



## Vibrational spectra of NdF<sub>3</sub> crystal

A.S. Oreshonkov<sup>1,2</sup>, A.S. Krylov<sup>1,2</sup>, N.P. Shestakov<sup>1,2</sup>, V. N. Voronov<sup>1</sup>, A.A. Ershov<sup>1,\*</sup>,

E.A. Strikina<sup>1</sup>, A.N. Vtyurin<sup>1,2</sup>

<sup>1</sup>*Kirensky Institute of Physics, SB RAS, 660036, Krasnoyarsk, Russia*

<sup>2</sup>*Siberian Federal University, 660079, Krasnoyarsk, Russia*

**Keywords:** trifluorides, tysonite structure, Raman spectroscopy, Infrared spectroscopy

**Running head:** Vibrational spectra of NdF<sub>3</sub> crystal

\* Corresponding author: *E-mail: ershov@iph.krasn.ru, Phone: +7 391 249 4510, Fax: +7 391 243 8923*

## Vibrational spectra of NdF<sub>3</sub> crystal

The vibrational spectroscopy investigation of phase transitions in NdF<sub>3</sub> crystal is reported. Spectra were obtained in temperature range from 300 to 10 K. It has been shown that, down to 10K, the orthorhombic tysonite structure of NdF<sub>3</sub> trifluoride remains stable.

### Introduction

The NdF<sub>3</sub> crystal belong to the rare-earth trifluoride crystals with the tysonite structure  $ReF_3$  ( $Re = La, Ce, Pr, Nd$ , space group  $P-3c1$ ,  $Z = 6$ ), which are extensively studied due to their wide applications in fiberoptics, as an active medium of solid-state lasers, sensors and scintillators [1-5]. Unit cell structure of NdF<sub>3</sub> crystal [6] is shown in Fig. 1. According to [7, 8]  $ReF_3$  crystals with tysonite structure undergoes a structural phase transition to high-pressure phase  $Cmma$  around 20 GPa. On the other hand, the quantum mechanical simulations [9] and in situ X-ray diffraction [10] shows less-distorted  $I4/mmm$  structure for high-pressure phase of LaF<sub>3</sub> crystal. The crystal structure of La, Ce, Pr and Nd trifluorides is stable until melting [10]. The melting point of NdF<sub>3</sub> crystal is 1410 K.

The aim of this work was to perform the investigation of vibrational spectra of NdF<sub>3</sub> crystal in a wide temperature and pressure range looking for some features of structural phase transitions.

### Experimental

Single crystals of NdF<sub>3</sub> were grown by Bridgeman– Stockbarger method at the hot zone temperature 1400 C. The starting material was NdF<sub>3</sub> of spectral purity grade. The growth was performed in evacuated and sealed platinum ampoule. Temperature gradient inside the heater was 30 K/cm, and the pulling rate was 0.8 mm/hour. As-grown single

crystal samples were of several millimeter size and had several growth facets of rather high optical quality, the latter being varying for different facets. No strange reflections were observed with X-ray. Before measurement, as-grown crystals were polished to produce surfaces with perfect optical quality.

Raman spectra were collected using the polarized radiation of a 488 nm Ar<sup>+</sup> laser (Spectra-Physics Stabilite 2017) in the wavenumber region between 10 and 800 cm<sup>-1</sup>. The spectra were recorded on a Horiba Jobin Yvon T64000 spectrometer. The temperature studies were performed using an ARS CS204–X1.SS closed cycle helium cryostat in the temperature range of 13 – 300K. The accuracy of temperature stabilization during spectra measurement was <0.2 K. The samples for the far IR range was prepared by mixing of melted NdF<sub>3</sub> powder and polyethylene, pellet was made using pellet press. The spectra in the mid-IR range were collected from potassium bromide (KBr) pellet samples, KBr was used instead of polyethylene. The spectra were obtained with Vertex 80V IR spectrometer (Bruker). The temperature studies were performed using an Optistat<sup>TM</sup> AC-V cryostat in the temperature range of 10 – 286.

## Results and discussion

Mechanical representation of the  $P\bar{3}c1$  trigonal phase at Brillouin zone centre of NdF<sub>3</sub> crystal is:

$$\Gamma_{\text{Mech}} = 5A_{1g} + 5A_{1u} + 7A_{2g} + 7A_{2u} + 12E_u + 12E_g, \text{ acoustic and optic modes: } \Gamma_{\text{acoustic}} = A_{2u} + E_u,$$

$$\Gamma_{\text{optic}} = 5A_{1g} + 5A_{1u} + 7A_{2g} + 6A_{2u} + 11E_u + 12E_g, \text{ Infrared and Raman active modes } \Gamma_{\text{Raman}} = 5A_{1g} + 12E_g, \Gamma_{\text{Infrared}} = 6A_{2u} + 11E_u.$$

The Raman spectra and mid-infrared spectra of the NdF<sub>3</sub> crystal recorded at ambient condition are shown in Fig. 2 and the frequencies observed are listed in Table 1.

To calculate the NdF<sub>3</sub> vibrational spectrum we used simulation package LADY [11]. Complete spectra of the NdF<sub>3</sub> crystal obtained within the framework of simplified version of the Born-Karman model [12].

Within this model, only the pair-wise interactions and bond-stretching force constants  $A = \frac{\partial^2 E}{\partial R^2}$  ( $E$  – energy,  $R$  – bond length) are considered. Simplified version of the Born-Karman model implies that  $A$  depends on  $R$  and the  $A(R)$  dependencies are the same for all atom pairs:

$$A = \lambda \exp(-r_{ij}/\rho),$$

where  $r_{ij}$  is the interatomic distance, and  $\lambda$  and  $\rho$  are the parameters characterizing selected pair interaction. To find the parameters of the model the special optimization program was written and tested for several compounds [13-15]. The crystal lattice stability conditions were taken into account. The parameters obtained for NdF<sub>3</sub> crystal are shown in Table 2.

Temperature transformation of Raman spectra is shown in Fig. 3. Crystal cooling leads to reduction of line widths, and to the appearance of the line about 45 cm<sup>-1</sup>. According to the NdF<sub>3</sub> lattice dynamics calculations three  $E_g$  mode should appear in the region below 100 cm<sup>-1</sup>. Two of them are can be clearly seen in Fig. 3 at 36 and 75 cm<sup>-1</sup> at room temperature. Third line should exits near 50 cm<sup>-1</sup>. Thus, it can be assumed that the appearing of the line near 50 cm<sup>-1</sup> can be connected with it intensity increasing. No any significant changes in Raman spectra devoted to the structural phase transitions are observed. The IR spectra of the NdF<sub>3</sub> compound at different temperatures are shown in Fig. 4. It can be seen that, down to 10K, the infrared spectra do not exhibit noticeable changes that could be attributed to structural phase transitions too. Thus, it can be argued that the crystal structure is stable from 300 to 10K.

## **Conclusion**

As a result of these investigations, we can conclude that  $\text{NdF}_3$  crystal do not undergo the structural phase transitions in the temperature range 300–10K. No any significant changes in vibrational spectra devoted to the structural phase transitions are observed. The number of active spectral lines is an agreement with the selection rules and the lattice dynamics calculation.

## **Acknowledgements**

This study was partially supported by the Ministry of Education and Science of the Russian Federation and the “Krasnoyarsky regional fund of scientific support and scientific-technical activity”.

## References

- [1] A. Kaminskii, Laser Crystals, Berlin: Springer (1990)
- [2] S. Krause, W. Moritz and I. Grohmann, Sens. Actuators, B, 1994, 18, 148–154.
- [3] S. Ye, B. Zhu, J. Luo, J. X. Chen, G. Lakshminarayana and J. R. Qui, Opt. Express, 16, 8989 (2008)
- [4] A.A. Kalinkin, A.A. Kalachev, V.V. Samartsev, Laser Physics, 13, 1313 (2003).
- [5] F. Wang and X. G. Liu, Chem. Soc. Rev., 2009, 38, 976–989
- [6] E.M. Diniz, C.W.A. Paschoal, Solid State Communications, 136, 538 (2005)
- [7] T.I. Dyuzheva, L.M. Lityagina, G.B. Demishev, N.A. Dendeliani, Journal of Alloys and Compounds, 335, (2002), 59–61.
- [8] T.I. Dyuzheva, L.M. Lityagina, G.B. Demishev, N.A. Dendeliani, Inorganic Materials 39 (2003) 1198–1202.
- [9] B. Winkler, K. Knorr and V. Milman, J. Alloys Compd., 2003, 349, 111–113.
- [10] Wilson A. Crichton, P. Bouvier, B. Winkler and A. Grzechnik, Dalton Trans. 39, 4302 (2010)
- [11] Smirnov, M. B.; Kazimirov, V. Yu. *JINR communications E* **2001**,14-2001-159.
- [12] M. Smirnov, R. Baddour-Hadjean, Li intercalation in TiO<sub>2</sub> anatase: Raman spectroscopy and lattice dynamic studies, J. Chem. Phys. 121 (2004) 2348-2355.
- [13] A.S. Krylov, A.N. Vtyurin, A.S. Oreshonkov, V.N. Voronov, S.N. Krylova, Structural transformations in single crystal Rb<sub>2</sub>NaYF<sub>6</sub>: Raman scattering study, J. Raman Spectr. 44 (5) (2013) 763-769.
- [14] Y.V. Gerasimova, A.S. Oreshonkov, A.N. Vtyurin, A.A. Ivanenko, L.I. Isaenko, A.A. Ershov, E.I. Pogoreltsev, Imfrared absorption investigation of the role of

octahedral groups upon the phase transition in the  $\text{Rb}_2\text{KMoO}_3\text{F}_3$  crystal, *Phys. Solid State* 55 (11) (2013) 2331-2334.

- [15] Zhiguo Xia, M.S. Molochev, A.S. Oreshonkov, V.V. Atuchin, Ru-Shi Liu, Cheng Dong, Crystal and local structure refinement in  $\text{Ca}_2\text{Al}_3\text{O}_6\text{F}$  explored by X-ray diffraction and Raman spectroscopy, *Phys. Chem. Chem. Phys.* 16 (2014) 5952-5957.

**Fig. 1:** Structure of NdF<sub>3</sub> crystal: a) projection on the ab plane, b) perspective view

**Fig. 2:** The Raman spectra and mid-infrared spectra of the NdF<sub>3</sub> crystal

**Fig. 3:** Temperature transformation of Raman spectra of the NdF<sub>3</sub> crystal

**Fig. 4:** IR spectra of the NdF<sub>3</sub> crystal at different temperatures



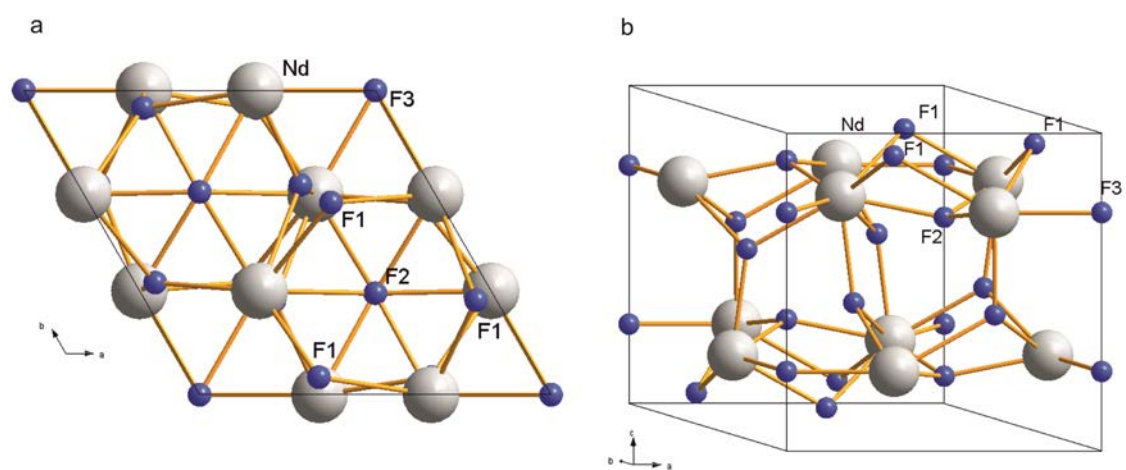


Fig.1.

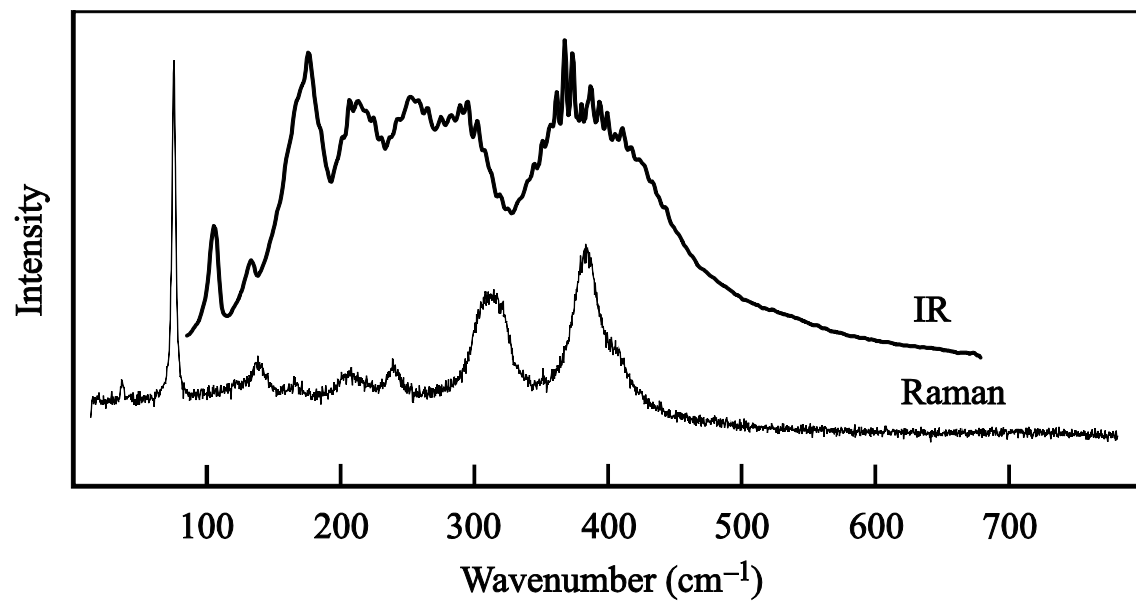


Fig.2.

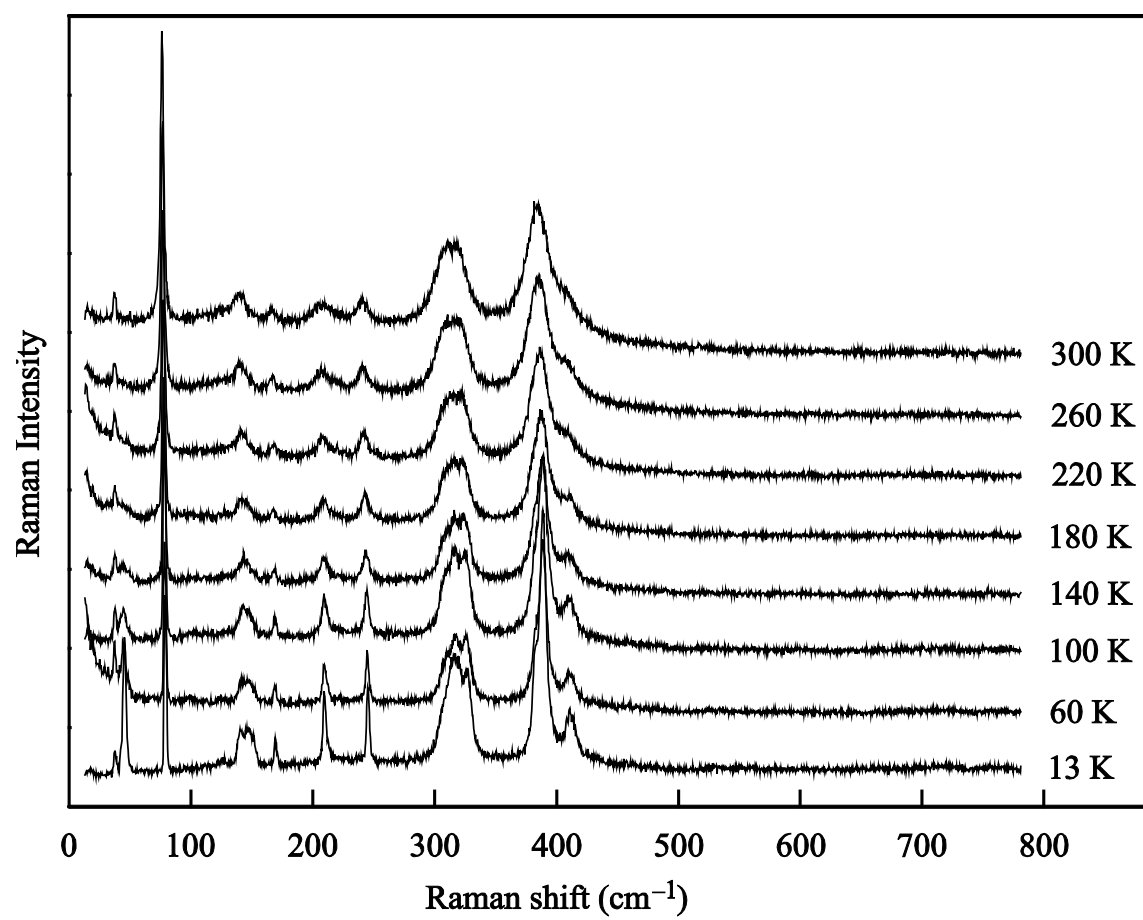


Fig. 3.

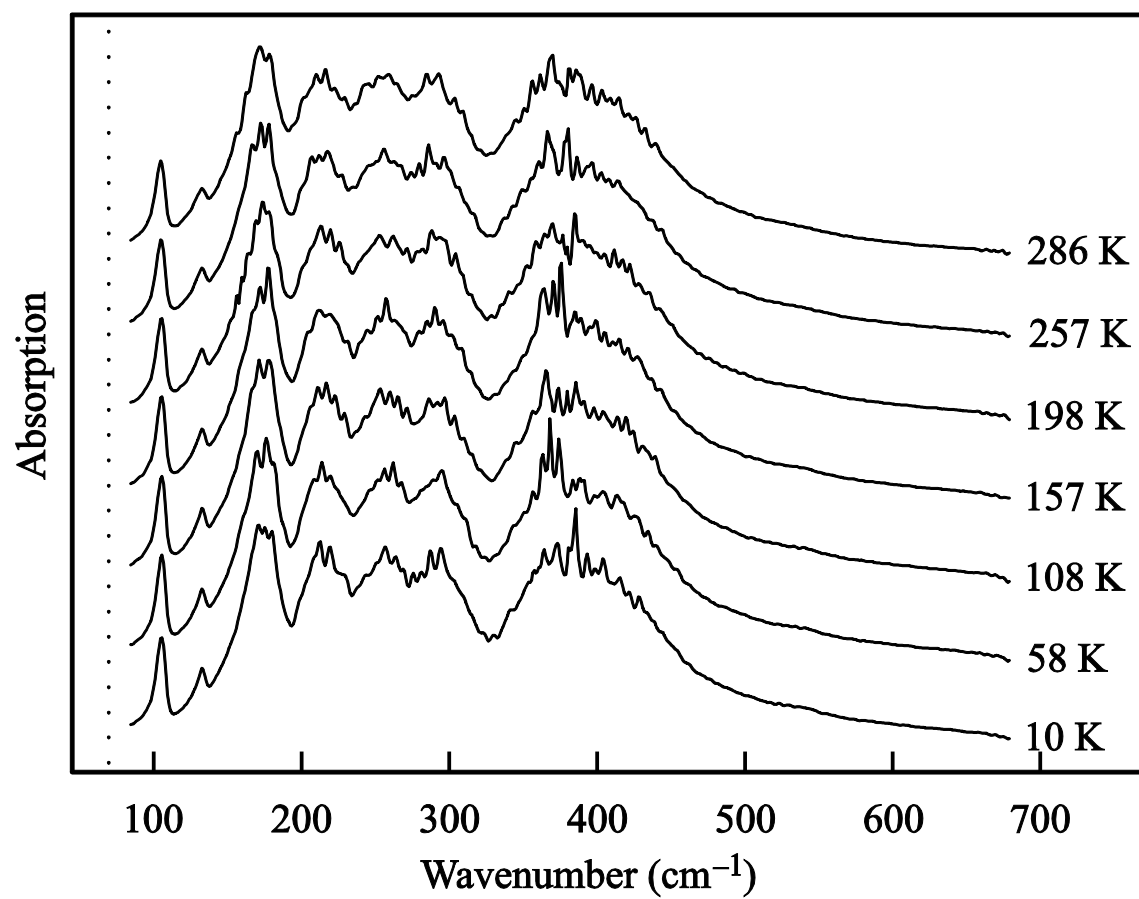


Fig. 4.

**Table 1:** Experimental and calculated Raman and Infrared frequencies, and band assignments for NdF<sub>3</sub> crystal.

**Table 2.** Parameters of the interatomic interaction potential.

Symm. Type	Raman exp 13K (cm <sup>-1</sup> )	Raman exp 300K (cm <sup>-1</sup> )	Raman calc. 300K (cm <sup>-1</sup> )	Symm. type	IR exp 300K (cm <sup>-1</sup> )	IR Calc 300K (cm <sup>-1</sup> )
$E_g$	37	36	36	$A_{2u}$		38
$E_g$	45		53	$E_u$	105	41
$E_g$	78	75	81	$E_u$	132	58
$A_{1g}$	123	120	84	$A_{2u}$		75
$A_{1g}$	140	138	129	$A_{2u}$	163	116
$E_g$	146		141	$E_u$	176	121
$E_g$	151		164	$A_{2u}$	212	137
$A_{1g}$	169	165	176	$E_u$		140
$E_g$	209	207	181	$E_u$	253	165
$E_g$	219		199	$E_u$		181
$E_g$	245	240	248	$E_u$	294	217
$A_{1g}$	308	306	295	$A_{2u}$		238
$E_g$	316		296	$E_u$	345	252
$E_g$	327	319	322	$E_u$	367	295
$E_g$	382		372	$E_u$	397	311
$E_g$	388	384	398	$A_{2u}$	432	336
$A_{1g}$	412	407	401	$E_u$		381

Table 1.

Interactions	$\lambda$ , aJ/Å <sup>2</sup>	$\rho$ , Å
Nd – F1	544.6	0.340
Nd – F2	321.6	0.286
Nd – F3	400.6	0.363
F1 – F1	345.3	0.379
F1 – F2	242.8	0.330
F1 – F3	196.8	0.323

Table 2.